Assessing the Dynamic Viscosity of Na–K–Ca–Cl–H2O Aqueous Solutions at High-Pressure and High-Temperature Conditions

ARTICLE *in* INDUSTRIAL & ENGINEERING CHEMISTRY RESEARCH · JUNE 2014

Impact Factor: 2.59 · DOI: 10.1021/ie501702z

6 AUTHORS, INCLUDING:

Hossein Safari

Research Institute of Petroleum Industry (RIPI)

12 PUBLICATIONS **42** CITATIONS

SEE PROFILE

I&EC research
Industrial & Engineering Chemistry Research

Article

pubs.acs.org/IECR

Assessing the Dynamic Viscosity of Na−K−Ca−Cl−H_2O Aqueous Solutions at High-Pressure and High-Temperature Conditions

Hossein Safari,*[,†] Sahand Nekoeian,[‡] Mohammad Reza Shirdel,[§] Hossein Ahmadi,[†] Alireza Bahadori,*[,⊥] and Sohrab Zendehboudi[¶]

[†]Department of Petroleum Engineering and [‡]Department of Chemical Engineering, Petroleum University of Technology, Ahwaz 63431, Iran

[§]Schlumberger Stimulation and Cementing Services, Kish Island 79417, Iran

[⊥]School of Environment, Science, & Engineering, Southern Cross University, Lismore, NSW 2480, Australia

[¶]Department of Chemical Engineering, Massachusetts Institute of Technology (MIT), Cambridge, Massachusetts 02139, United States

ABSTRACT: Most industrial areas, especially oilfield operations and geothermal reservoirs, deal with varying viscosities in multicomponent electrolyte solutions. An accurate estimate of this property as a function of pressure, temperature, and varying salt concentrations is highly desirable. Although a number of empirical correlations have already been developed, they are still limited to single electrolyte solutions and can only operate over specified temperature and pressure ranges. In this study, a highly accurate model based on an adaptive network-based fuzzy inference system was developed, mainly devoted to dynamic viscosity prediction in aqueous multicomponent chloride solutions. Crisp input data were transformed into fuzzy sets employing the subtractive clustering algorithm with an effective radius optimized by a hybrid of genetic algorithm and particle swarm optimization technique. Comparing the model with thousands of experimental data concluded in squared correlation coefficient (R^2) of 0.9986 and an average absolute error of 1.59%. The developed model was also found to outperform a number of empirical correlations that are employed for the viscosity determination of single electrolyte solutions.

1. INTRODUCTION

Knowledge of the thermo-physical and transport properties of aqueous electrolyte solutions is considered of paramount importance in a variety of applications in chemical, mechanical, and petroleum engineering. As a crucially important transport property, viscosity plays a vital role in geothermal applications, oilfield operations, desalination units, and many other industrial processes that deal with fluid−rock interactions, fluid-flow simulations, material transport, fluid-inclusion studies, and liquid-dominated systems.[1−3]

Geothermal heat and power plants employ hot geothermal fluids as transport media for extracting energy from underground formations.[1] The complex nature of the fluids in geothermal reservoirs and the presence of different ions in water as a result of water−rock interactions necessitate the contribution of many disciplines in science and engineering for the numerical or analytical modeling of fluid flow through porous media. Efficient development of geothermal reservoirs relies on the accurate measurement of reservoir rock and fluid properties together with the interpretation of methods for implementation of measured data.

Because of the temperature degradations of fluids from higher degrees existing in underground formations to lower degrees at the surface either around production or injection wells or in surface facilities, no uniform viscosity could be assumed in engineering calculations of well productivity or flowline computations.[4] A literature survey by Ophori[5] shows that most numerical models have considered the impact of density while the variation in the viscosity of underground formation water is neglected. Yet, other studies suggest that there is a strong relationship between viscosity and density and therefore assuming a constant viscosity is highly prone to cause incorrect simulation results.[6] The significance of viscosity has also been highlighted in the works of Magri et al.,[7] Yidana,[8] and Mark Yidana et al.[9]

Proper knowledge of the relationship between the viscosity of aqueous solutions and important thermodynamic characteristics (e.g., temperature, pressure, and composition) happens to be extremely important in petroleum engineering calculations as well. The recovery of hydrocarbons in an underground reservoir is usually accompanied by the production of water trapped in rock pores. The density and salinity of this water could be comparably higher than those of seawater.[10] An accurate estimate of the water dynamic viscosity under wide ranges of temperature, pressure, and ionic compositions is indispensible in optimal production design and reservoir engineering calculations.[4]

Most petroleum reservoirs are generally surrounded by saline aquifers, which may act as their driving forces during the primary stages of production. Secondary recovery techniques, the most important of which is water flooding, are usually implemented after the reservoir is depleted and natural production mechanisms are no longer active.[11] Likewise, the transport properties of

Received: April 25, 2014
Revised: June 6, 2014
Accepted: June 10, 2014

   dx.doi.org/10.1021/ie501702z | *Ind. Eng. Chem. Res.* XXXX, XXX, XXX−XXX

Table 1. Summary of Dynamic Viscosity Measurements

author(s)	method[a]	uncertainty (%)	T (K)	P (MPa)	compositions (m)
Korosi and Fabuss[17]	CMGC	0.1−0.2	298.15−423.15	0.1	NaCl (0−3.6)
					KCl (0−3.6)
Korosi and Fabuss[37]	GCV	0.2	298.15−423.15	0.1	pure water
Kestin, H. and R.[13]	ODV	0.5	298.15−423.15	0.1−35	KCl (0−5)
Kestin, H. and R.[12]	ODV	1	293.15−423.15	0.1−35	NaCl (0−6)
Ershaghi, Abdassah, Bonakdar, and Ahmad[4]	CF	n.a.[b]	298.15−260	0.1	NaCl (0−3.5)
					KCl (0−2.75)
					$CaCl_2$ (0−1.84)

[a]CMGC, Cannon Master glass capillary; GCV, glass capillary viscometer; ODV, oscillating-disc viscometer; CF, capillary flow method. [b]n.a., not available.

aqueous solutions including viscosity are undoubtedly requisite for simulating the phase behaviors and possible interactions of injected water and indigenous formation water under reservoir conditions.

Experimentalists have carried out a large number of laboratory work and over thousands of dynamic viscosity measurements have been reported by different researchers. We have collected the viscosity data of ($NaCl+H_2O$), ($KCl+H_2O$), ($CaCl_2+H_2O$) systems. The authors' names, published year, and uncertainty values together with the operating ranges are summarized in Table 1. The available databases for NaCl and KCl solutions are quite large compared to the other electrolyte solutions, and Kestin and co-workers[12,13] had the most contribution to these viscosity measurements. The gathered experimental data are still scattered and only cover certain ranges of temperature, pressure, and salt concentration. To this end, a number of researchers have devoted extensive attempts to providing theoretical models so as to interpolate the data points among these ranges.

Numbere et al.[14] proposed an empirical correlation for the dynamic viscosity of the salt-containing water phase, which is only applicable to sodium chloride solutions and requires the viscosity of pure water to be known at the same operating conditions. It appears that this correlation might not be a suitable choice for engineering calculations and has not been employed much by researchers. Ershaghi, Abdassah, Bonakdar, and Ahmad[4] also developed an empirical correlation for the dynamic viscosity of NaCl containing solutions using the data measured in their own work. Nevertheless, this correlation does not account for the effect of pressure and only covers a temperature range of 50−275 °C.

The most exhaustive equation for the prediction of the dynamic viscosity of single electrolyte solutions could be found in the study of Kestin and colleagues.[12,13] This correlation takes into account the influence of pressure as well as temperature for $NaCl+H_2O$ and $KCl+H_2O$ binary systems. In the following, some of the important dynamic viscosity correlations will be described in detail.

1.1. Dynamic Viscosity Correlations. *1.1.1. Ershaghi, Abdassah, Bonakdar, and Ahmad.*[4] In their attempt to measure the dynamic viscosity of NaCl, KCl, and $CaCl_2$ aqueous solutions at elevated temperatures, Ershaghi, Abdassah, Bonakdar, and Ahmad[4] presented an analytical expression to describe the viscosity data of NaCl containing solutions. This correlation is written as follows:

$$\mu = 10^{-4}[\alpha + \beta T + \gamma T^2 + \delta T^3 + 241.4 \times 10^{247.8/(T-140)}] \quad (1)$$

in which T is the temperature in K, and α, β, γ, and δ are concentration-dependent constants that are described as follows:

$$\alpha = 0.7543564 \times 10^4 + 0.1585416 \times 10^4 C - 0.2153238 \times 10^3 C^2 + 0.1311786 \times 10^2 C^3 \quad (2)$$

$$\beta = -0.4203004 \times 10^2 - 0.8313187 \times 10^1 C + 0.1260422 \times 10^1 C^2 - 0.7739334 \times 10^{-1} C^3 \quad (3)$$

$$\gamma = 0.81770676 \times 10^{-1} + 0.1507287 \times 10^{-1} C - 0.2354586 \times 10^{-2} C^2 + 0.1479379 \times 10^{-3} C^3 \quad (4)$$

and

$$\delta = -0.5509047 \times 10^{-4} - 0.8906202 \times 10^{-5} C + 0.1396191 \times 10^{-5} C^2 - 0.9156521 \times 10^{-7} C^3 \quad (5)$$

where C is the concentration of NaCl salt in weight percentage. The developed model is applicable within the temperature interval of 50−275 °C. This equation can be also applied to geothermal brines that contain other salts provided that their equivalent NaCl concentration is calculated using the multipliers given in the work by Ershaghi, Abdassah, Bonakdar, and Ahmad[4]. However, these multipliers are only limited to certain ranges of temperature and concentration.

1.1.2. Kestin and Co-Workers.[12,13] The viscosity correlation proposed by Kestin et al.[12,13] is presented by the following form:

$$\mu(P, T, C) = \mu^\circ(T, C)[1 + \beta(T, C)P] \quad (6)$$

where μ stands for the dynamic viscosity in μPa·s, P is pressure in MPa, T is temperature in °C, and C refers to the salt concentration (either NaCl or KCl) in molality (m). The hypothetical zero-pressure viscosity (μ°) is given by

$$\mu^\circ(T, C) = \mu_w^\circ(T)\left[1 + \sum_{i=0}^{2}\sum_{j=0}^{2} A_{ij} C^{j+1} T^i\right] \quad (7)$$

where μ_w° is the hypothetical zero-pressure dynamic viscosity introduced by Kestin et al.:[15]

$$\log_{10}[\mu_w^\circ(T)/\mu_w^\circ(20\ ^\circ\mathrm{C})] = \frac{\sum_{i=1}^{4} \alpha_i (20 - T)^i}{90 + T} \quad (8)$$

where α_1−α_4 are equal to 1.2378, 1.303×10^{-3}, 3.06×10^{-6}, and 2.55×10^{-8}, respectively. The measurement of viscosities is almost universally based on the absolute value of water viscosity at 20 °C as a primary standard.[16] This parameter was

dx.doi.org/10.1021/ie501702z | Ind. Eng. Chem. Res. XXXX, XXX, XXX−XXX

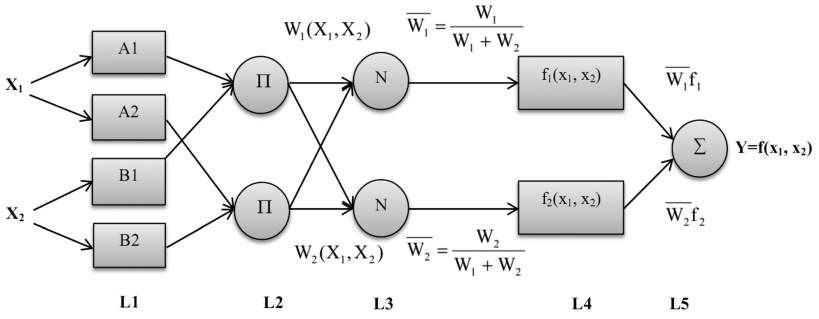

Figure 1. A typical schematic of the ANFIS structure for a two-input problem.

determined by Swindells, Coe, and Godfrey[16] to be around 1002 μPa·s.

The pressure coefficient (β) in eq 6 appears as a linear factor, which can be calculated according to the following formula:

$$\beta(T, C) = \beta_s^E \beta^*(C/C_s) + \beta_w(T) \tag{9}$$

where the pressure coefficient of water (β_w) is defined by

$$\beta_w(T), \text{ GPa}^{-1} = \sum_{i=0}^{4} b_i T^i \tag{10}$$

The excess pressure coefficient (β_s^E) at salt saturation is only a function of temperature and can be computed using the following expression:

$$\beta_s^E(T), \text{ GPa}^{-1} = \lambda_1 + \lambda_2 T - \beta_w(T) \tag{11}$$

The concentration of salts at their saturation is expressed by

$$C_s(T) = \sum_{i=0}^{2} \theta_i T^i \tag{12}$$

In addition, the reduced excess pressure coefficient (β^*) is obtained by the following equation:

$$\beta^*(C/C_s), \text{ GPa}^{-1} = \sum_{i=1}^{3} \gamma_i (C/C_s)^i \tag{13}$$

In these equations, A, α, b, λ, θ, and γ are all constants or vectors of constant parameters that are specific to a certain single electrolyte system, which can be obtained through multiple regression analyses. These parameters for KCl and NaCl were determined in the research study of Kestin, H. and R.[12,13] Although this correlation takes into account the pressure effect as compared to the correlation of Ershaghi, Abdassah, Bonakdar, and Ahmad,[4] the results obtained in the work of Korosi and Fabuss[17] suggest that pressure has a rather negligible effect on the dynamic viscosity as long as the pressure is lower than 200 psig. This is probably the most comprehensive dynamic viscosity correlation presented so far, which can be extended to any electrolyte system aside from KCl and NaCl under the circumstances that enough experimental data are available; however, for some specific salts such as $MgSO_4$, the experimental data reported in the open sources are scarce and the aforementioned parameters are rather unidentifiable considering this data shortage.[18]

The methodologies introduced so far appear to work well within wide temperature and pressure ranges but are still limited to single electrolyte systems. This fact could be attributed to the high costs associated with the design of experiments for measuring the dynamic viscosity in complex systems in which a large number of components may exist. To address these problems, new methodologies must be developed that are capable of modeling precise viscosity values and take into consideration the concentrations of different salts in solution.

Inductive machine learning algorithms as branches of artificial intelligence have already been applied in providing applicable solutions to a wide variety of industrial and scientific problems.[19,20] This study employs a fusion of two soft computing techniques, namely artificial neural networks and fuzzy logic (FL), which is generally referred to as an adaptive network based fuzzy inference system (ANFIS). The notion behind this methodology lies in the fact that artificial neural networks can learn the patterns within data, whereas fuzzy logic can turn the observed patterns into linguistic if−then rules that are more comprehensible than the patterns observed by neural networks. Information regarding the fuzzy systems and the ANFIS structure will be described shortly within this study. The developed model is capable of accurately determining the dynamic viscosity in multicomponent (Na, K, or Ca)Cl−H_2O systems over temperatures varying between 293.15 and 533.15 K and pressure ranging from 0.1 to 35 MPa.

2. ADAPTIVE NETWORK BASED FUZZY INFERENCE SYSTEM (ANFIS)

The complexity and heterogeneity of real systems have rendered the call for more sophisticated and more error tolerant modeling techniques.[21] Modeling complicated systems with exact and conventional mathematical tools may not be very well suited considering the natural uncertainties associated with these systems.[21−23] In recent years, soft computing techniques such as artificial neural networks (ANNs) and fuzzy systems have successfully been applied in the robust modeling of complex real world problems.[22,24,25]

While debate exists regarding the precise definition of soft computing, the stance adopted in this paper is that given by Zadeh as follows:[21] "Soft computing differs from conventional (hard) computing in that, unlike hard computing, it is tolerant of imprecision, uncertainty, and partial truth". The concept of fuzzy logic was introduced by Zadeh[26] for modeling uncertain systems. In contrast to classical logic, which is based on crisp systems of true and false, fuzzy logic perceives the problems as a degree of truth (defined as the membership degree in fuzzy sets) or fuzzy sets of true and false.[26]

Modeling based on fuzzy logic is carried out using linguistic fuzzy if−then rules which provide an extraordinary method for qualitative process description without implementing precise quantitative measures; however, designing such models requires the proper and adequate knowledge about the problem being considered.[23]

dx.doi.org/10.1021/ie501702z | Ind. Eng. Chem. Res. XXXX, XXX, XXX−XXX

In most cases, the expert knowledge used as the basis of designing fuzzy systems is inadequate or uncertain, mainly owing to an incompleteness of existing knowledge and different biases of human experts. This is where data-driven soft computing techniques such as ANNs may be thought of as great alternatives since they can learn the required knowledge from available databases.[23] Fuzzy logic can be subsequently implemented to describe the learned patterns in linguistic if−then rules that are easy to comprehend. In fact, ANN and FL can be looked upon as complementary methods.

The cardinal part of ANFIS comes from a common framework referred to as adaptive networks, which combines both fuzzy models and neural networks. Fuzzy inference systems (FISs) can serve as the basis for defining a set of fuzzy if−then rules and membership functions (MFs), which are then fine-tuned using the learning capabilities of intelligence systems (e.g., ANNs).[22,23] Owing to the fact that ANFIS can achieve a successful nonlinear mapping of input−output data pairs, it is then very well suited for the problem of modeling the viscosity for multicomponent aqueous mixtures.

Two types of FIS structures have been proposed in the literature, namely Mamdani and Takagi−Sugeno−Kang (TSK).[23] While the former deals with a subjective definition of fuzzy if−then rules using expert statements, the latter provides a framework for generating these rules from input and output numerical data. Owing to the fact that a subjective definition of fuzzy rules may bring in vagueness and imprecision, ANFISs utilize the TSK fuzzy structures for successful nonlinear mapping of input and output patterns.[21−23]

Figure 1 represents a constructed ANFIS for a two-input system. In this figure, β functions represent the degrees of membership of each variable in the constructed fuzzy sets, X_1 and X_2 indicate the inputs, and Y is the output. Assuming a first order TSK FIS, a fuzzy model can be generated according to the following rules:[23]

Rule I:

$$\text{IF } \langle X_1 \text{ is } A_1 \text{ and } X_2 \text{ is } B_1 \rangle \text{ THEN } \langle f_1 = m_1X_1 + n_1X_2 + r_1 \rangle \tag{14}$$

Rule II:

$$\text{IF } \langle X_1 \text{ is } A_2 \text{ and } X_2 \text{ is } B_2 \rangle \text{ THEN } \langle f_2 = m_2X_1 + n_2X_2 + r_2 \rangle \tag{15}$$

Rule III:

$$\text{IF } \left\langle X_1 \text{ is } A_1 \text{ and } X_2 \text{ is } B_2 \right\rangle \text{ THEN } \left\langle f_3 = m_3X_1 + n_3X_2 + r_3 \right\rangle \tag{16}$$

Rule IV:

$$\text{IF } \left\langle X_1 \text{ is } A_2 \text{ and } X_2 \text{ is } B_1 \right\rangle \text{ THEN } \left\langle f_4 = m_4X_1 + n_4X_2 + r_4 \right\rangle \tag{17}$$

where $A_{1,2}$ and $B_{1,2}$ are respective fuzzy sets of X_1 and X_2. Conditions stipulated in the IF part are generally known as antecedent, and those in the THEN part are called the consequence. According to Lee,[23] a typical ANFIS is normally composed of five different layers.

Layer 1. In this layer, crisp input data given into the system are converted into fuzzy numbers or linguistic terms. For example, in the schematic diagram shown in Figure 1, X_1 and X_2 are both connected to two nodes, meaning that two linguistic terms or fuzzy sets have been defined for each of these inputs. This step, which is also referred to as the fuzzification layer, constructs fuzzy sets based on predefined MFs. Although the selection of the MF is not limited and is more of a case-dependent issue, Gaussian MFs are more preferred for nonlinear regression problems because they lead to a smooth model behavior. Gaussian MFs implemented in this study are defined according to the following expression:

$$O_i^1 = \beta(X) = \exp\left(-\frac{1}{2}\frac{(X - Z)^2}{\sigma^2}\right) \tag{18}$$

in which O represents the layer outputs, Z defines the Gaussian center, and σ^2 stands for the variance. Gaussian parameters are finally tuned by the ANFIS to obtain more robust and accurate predictions.

Layer 2. This layer calculates the degree of correctness or applicability of the statements stipulated in antecedent parts, which is also called the firing strength, according to the following relationship:[23]

$$O_i^2 = W_i = \beta_{Ai}(X)\cdot\beta_{Bi}(X) \tag{19}$$

Layer 3. Each of the firing strengths calculated in the previous layer (W_i), are normalized in this layer to make a distinction between the firing strength of each rule and the entire firing strengths of all rules as given below:

$$O_i^3 = \frac{W_i}{\sum_i W_i} \tag{20}$$

Layer 4. Like the first layer, nodes of this layer (also known as the consequent layer) represent the linguistic terms of the output variable (which is the viscosity of aqueous solutions in the current study). The contribution of each rule toward the total output is described as

$$O_i^4 = \overline{W}_i f_i = \overline{W}_i(m_iX_1 + n_iX_2 + r_i) \tag{21}$$

where m_i, n_i, and r_i are called consequent or linear parameters. These parameters, along with the parameters mentioned in the first layer, are tuned during the learning process to attain a better match between real targets and ANFIS outputs.

Layer 5. This layer is called the defuzzification layer where the total number of rules defined for one output are aggregated and defuzzified into numerical outputs through a weighted average sum given below:

$$O_i^5 = Y = \sum_i \overline{W}_i f_i = \overline{W}_1 f_1 + \overline{W}_2 f_2 = \frac{\sum_i W_i f_i}{\sum_i W_i} \tag{22}$$

3. BUILDING THE ANFIS MODEL FOR DYNAMIC VISCOSITY PREDICTION

3.1. Data Acquisition and Statistical Summary. To build a reliable and accurate model capable of predicting the viscosity of aqueous electrolyte solutions at high temperatures and pressures, comprehensive (covering wide ranges of operational conditions) and accurate experimental data are required. To this end, an aggregate number of 5537 published data were gathered from the open literature to assemble an exhaustive database. According to the references provided in Table 1, water viscosity appears to be a function of temperature, pressure, and strong electrolyte concentrations in water as expressed below:

dx.doi.org/10.1021/ie501702z | Ind. Eng. Chem. Res. XXXX, XXX, XXX−XXX

Table 2. Statistical Description of Collected Database

parameters	minimum	maximum	average	standard deviation
temperature, K	293.15	533.15	362.90	43.6816
pressure, MPa	0.1	35	16.12	11.9439
C_{NaCl}, m	0	6	1.58	2.0008
C_{KCl}, m	0	5	1.07	1.5972
C_{CaCl_2}, m	0	1.84	0.02	0.1647
viscosity (μ_w), cp	0.11	1.99	0.52	0.2975

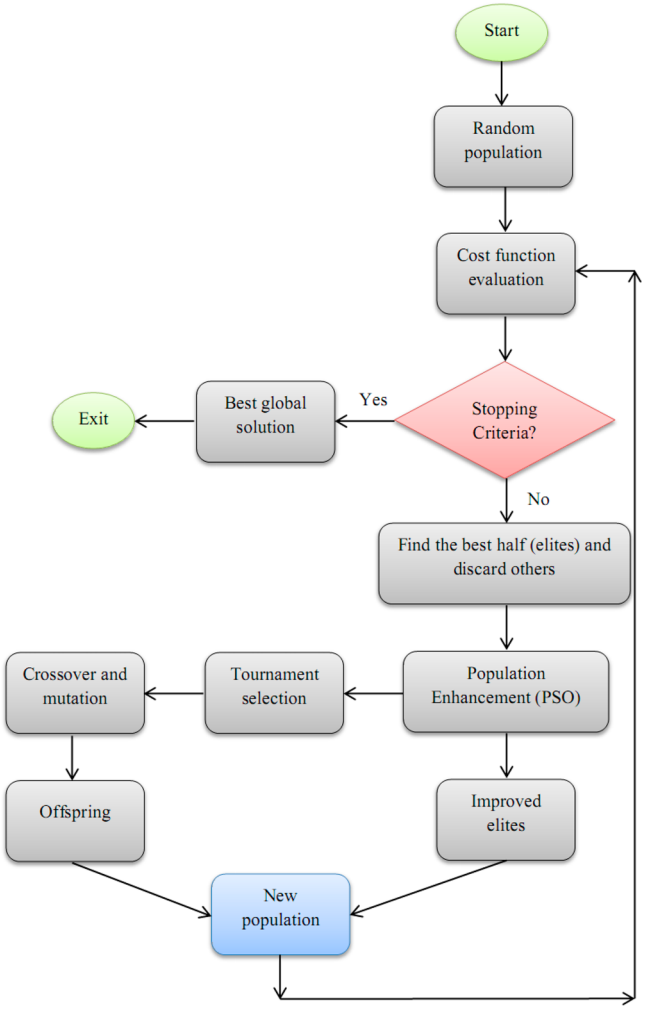

Figure 2. A typical flowchart of the HGAPSO optimization algorithm.[29]

$$\mu_w = f(T, P, C_{NaCl}, C_{KCl}, C_{CaCl_2}) \quad (23)$$

The assembled data set was initially divided by performing a random permutation into three subsets, namely "train," "check," and "test". To increase the model applicability and robustness and to reduce the chance of bias in the connectionist model, the collected database was divided randomly into 70%, 15%, and 15% fractions for the train set (3876), check set (831), and test set (830), respectively. The train set was used to train the model to capture the dominant patterns among the data; the series of check data was used to evaluate the model performance during the learning process to ascertain that overfitting would not occur; and finally, the test phase was conducted to evaluate the model generalization capability for unseen data after its successful training process. The statistical information

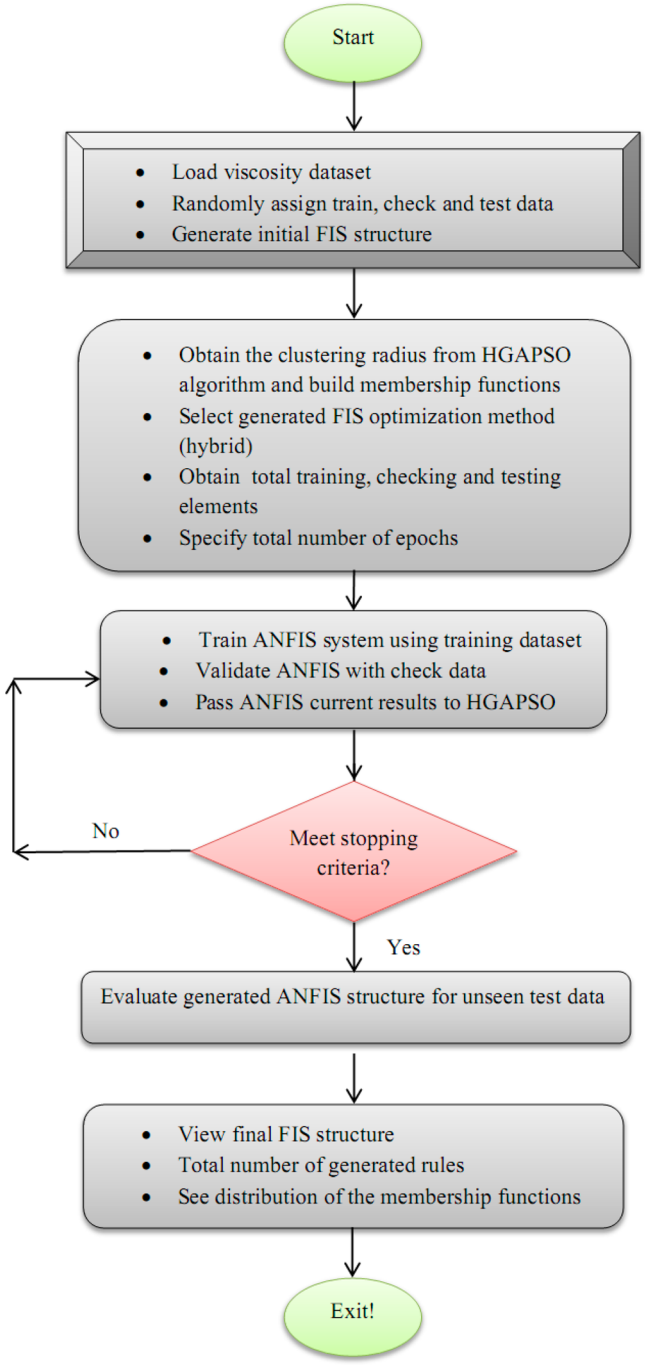

Figure 3. A simple flowchart of the top-down design algorithm for dynamic viscosity prediction using the ANFIS.

such as the ranges of input variables, minimum, maximum, and so on are tabulated in Table 2.

3.2. Model Development and Optimization. A number of methods are available for fuzzifying the crisp input data, namely the lookup table method, fuzzy c-means (FCM), and subtractive clustering (SC). The first method is not recommended for large scale problems because of the increased number of model parameters and MFs, which leads to heedless system complexity.[23]

The SC and FCM methods are clustering algorithms that are used extensively not only for data organization and categorization but also in useful data compression for ANFIS model development. Although both methods are superior compared

dx.doi.org/10.1021/ie501702z | Ind. Eng. Chem. Res. XXXX, XXX, XXX−XXX

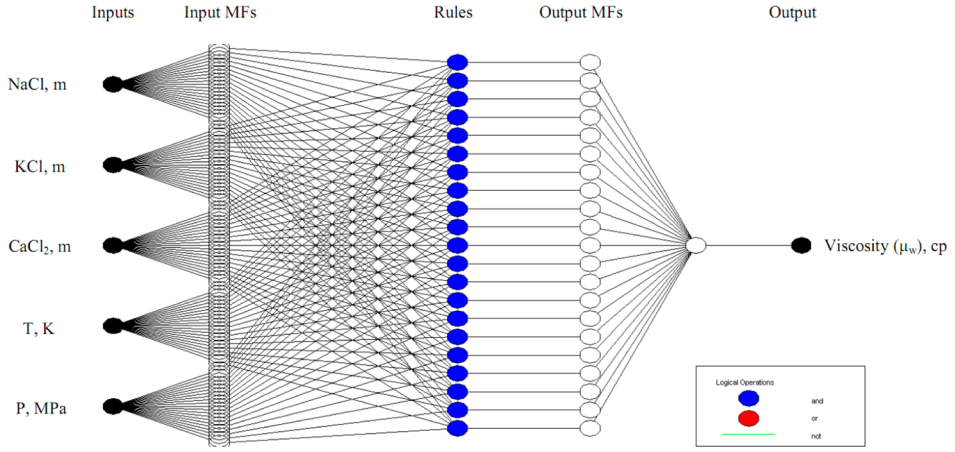

Figure 4. ANFIS structure for estimation of the dynamic viscosity of aqueous solutions.

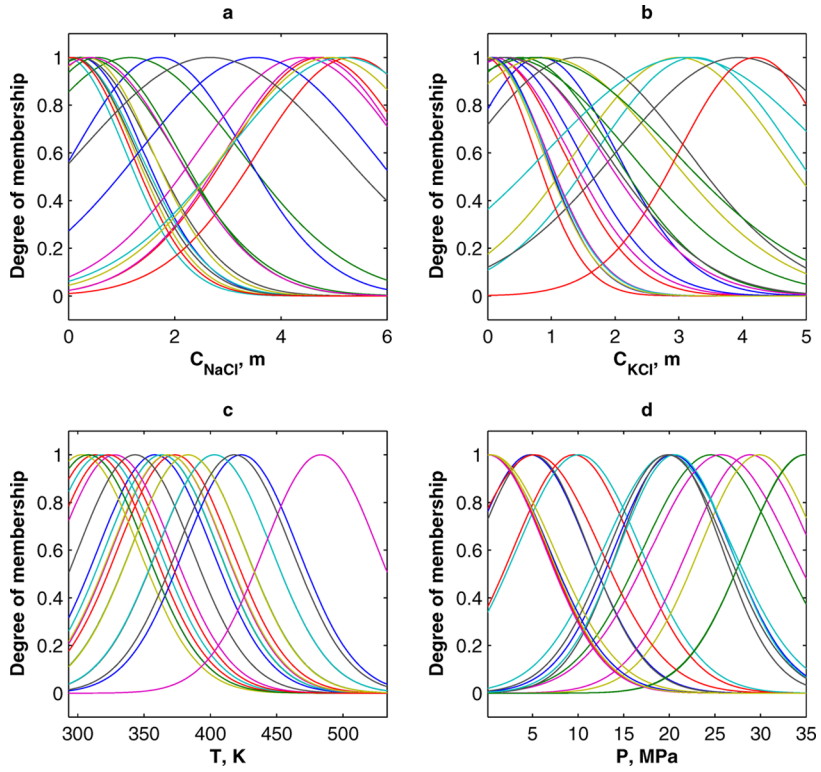

Figure 5. MFs generated by the SC algorithm for (a) NaCl, (b) KCl, (c) temperature, and (d) pressure.

to lookup table methodology, most studies have preferred SC over the FCM method.[21−23]

FCM is a clustering method in which each data belongs to a cluster with a degree specified by its MF. The center of the clusters is found in an iterative process during which the value of an objective function known as mountain function is minimized within a number of epochs. Nevertheless, computations grow exponentially with the increasing dimension of the problem, mainly because the algorithm evaluates the mountain function over all of the grid points.[22] The SC method proposed by Chiu[27] was utilized in this study because of its simple calculation procedure and its independence of the problem dimensionality.

Despite FCM, the SC method considers the data points as cluster centers instead of grid points with an effective cluster radius.[22] This effective radius was optimized in this work by the employment of the hybrid of the genetic algorithm (GA) and particle swarm optimization (PSO), generally known as the HGAPSO algorithm.

3.3. Hybrid of Genetic Algorithm and Particle Swarm Optimization (HGAPSO). *3.3.1. Genetic Algorithm (GA).* The GA is one of the evolutionary optimization techniques developed by John Holland over the course of the 1960s and 1970s and is based on the genetic theory and natural selection.[28] In a search for the optimum solution, the GA constructs a candidate list of solutions to the problem, which are referred to as individuals or chromosomes. Each individual represents a point in the search domain and thus holds a list of candidate solutions.[29]

Each solution could be encoded as a binary string of real-valued coefficients, which are then evaluated using a performance function (or objective function). Wright[30] claimed that the use of real-valued genes offers a number of advantages in numerical function optimizations over binary encodings. In fact,

dx.doi.org/10.1021/ie501702z | Ind. Eng. Chem. Res. XXXX, XXX, XXX−XXX

the real-valued GA tends to be inherently faster than the binary GA because the chromosomes do not need to be decoded prior to the objective function (or cost function in minimization problems) evaluation.[28] Individuals in the population are then sorted according to their costs and then, usually with the use of a selection algorithm, random pairs of better individuals are selected and a new population is reproduced using GA basic crossover and mutation operators.

The crossover operator produces two offspring (two new individuals) through recombining the genetic information of the parents.[29] The mutation is applied to alter the genetic structure of the individuals within chromosomes and to avoid the problem of fast convergence to local minima by introducing some changes to the genes or variables.[28,31]

3.3.2. Particle Swarm Optimization (PSO). Particle swarm optimization is one of the latest evolutionary optimization techniques, developed by Eberhart and Kennedy,[32] which is inspired by the coordinated motion of animals such as bird flocking or fish schooling. Like the GA, PSO is a population-based stochastic algorithm that is initialized with random initial populations possessing random positions and random velocities in a multidimensional search space.

The particles, which are also the candidate solutions to the optimization problem, fly around in the search space in an effort to find the optimum solution. The theory of PSO describes an iterative solution process in which each particle's velocity and position in space is constantly updated according to previous best performance of the particle or its neighborhood (i.e., cognitive behavior), as well as the best performance of the particles in the entire population (i.e., social behavior). The PSO algorithm can be formulated as follows:[33]

$$v_i^{j+1} = w^j v_i^j + c_1 \alpha_1{}^j (\mathrm{Pb}_i^j - x_i^j) + c_2 \alpha_2{}^j (\mathrm{Gb}_i^j - x_i^j) \quad (24)$$

$$x_i^{j+1} = x_i^j + v_i^{j+1} \quad (25)$$

where v_i^j and x_i^j represent velocity and position vectors of the ith particle at iteration j, respectively. Pb_i is the personal best of each individual in the population, while Gb_i is the global best position found in the entire population. The parameters $\alpha_{1,2} \in [0,1]$ are vectors of uniformly distributed random numbers, $\alpha_{1,2}$ are acceleration constants, and w is called the inertia weight.

Inertia weight was introduced by Shi and Eberhart[34] into eq 24 in order to dampen the natural tendency of standard PSO to explode at higher oscillations. Reducing w over time results in a shift from an exploratory to an exploitative search further guaranteeing convergence toward the global minima. In general, w reduces linearly with the iteration number, from w_{initial} to w_{final}:[34]

$$w^j = \frac{(j_{\max} - j) \times (w_{\mathrm{initial}} - w_{\mathrm{final}})}{j_{\max}} + w_{\mathrm{final}} \quad (26)$$

in which $j_{\max}$ indicates the maximum number of iterations performed. A good starting point would be to set w_{initial} to 0.9 and w_{final} to 0.4.[33]

3.3.3. HGAPSO Algorithm. Compared to the GA, PSO has a number of appealing characteristics. PSO is probably the only evolutionary algorithm that does not employ survival of the fittest;[33] therefore, both low- and high-value individuals survive during the search and could explore any point in the feature space.[35] Thus, in PSO, knowledge of good solutions is retained by all particles during the construction of several generations, and no information is discarded as compared to GA.

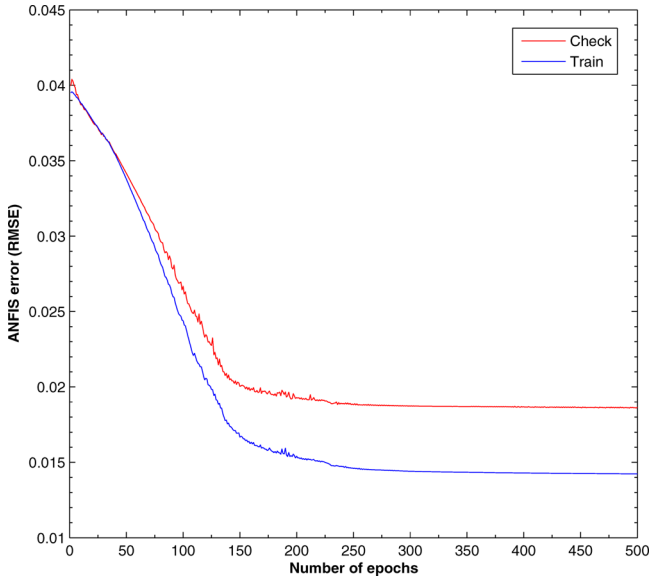

Figure 6. Plot of ANFIS errors versus total number of epochs.

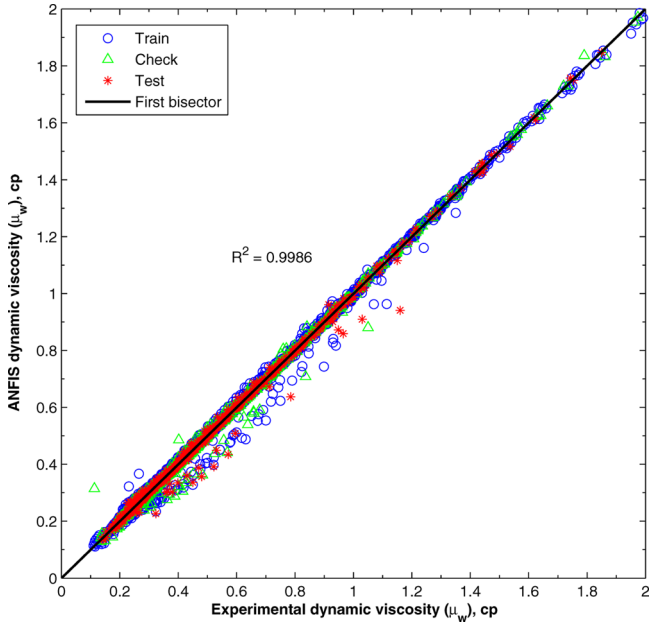

Figure 7. Regression plot of ANFIS predictions of viscosity values versus observed values.

Information sharing mechanisms are also completely different.[35,36] Information in PSO is only disseminated by a global best particle and thus is directional; nevertheless, in the GA, this information is shared among all chromosomes and the whole population moves toward the optimum solution.[29]

In general, all individuals in PSO belong to the same generation, and optimization proceeds on the basis of the social adaptation of knowledge. On the other hand, the GA operates on the basis of evolution from one generation to the other, and individual adaptations in a single generation are not considered.[29] It appears that a hybridization of the GA and PSO could compensate for the deficiencies associated with each algorithm. In the GA, individuals are reproduced or selected as elite parents for the next generation without being enhanced; however, all of the individuals in nature adapt to the surrounding environment as they grow up prior to producing

dx.doi.org/10.1021/ie501702z | Ind. Eng. Chem. Res. XXXX, XXX, XXX−XXX

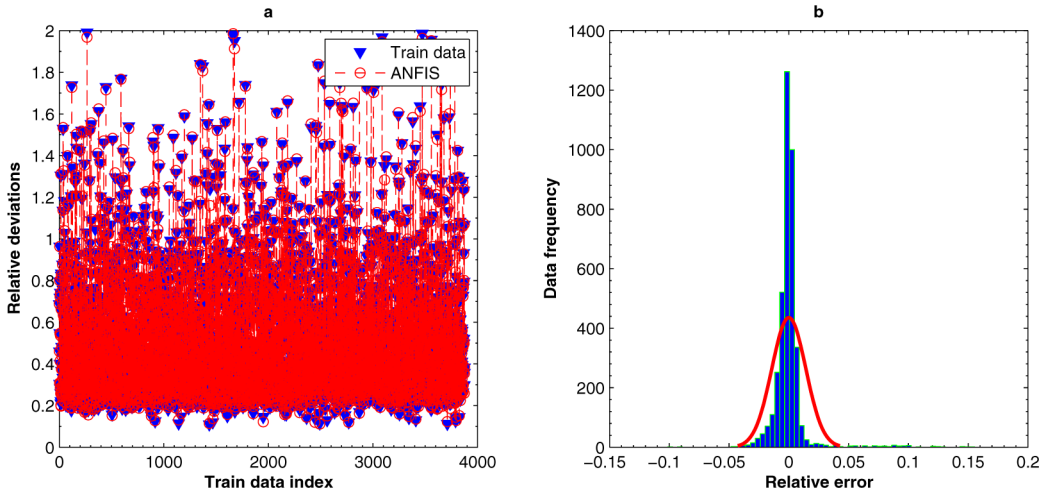

Figure 8. Deviations of ANFIS predictions from experimental data for the train set: (a) relative deviations, (b) error distributions histogram.

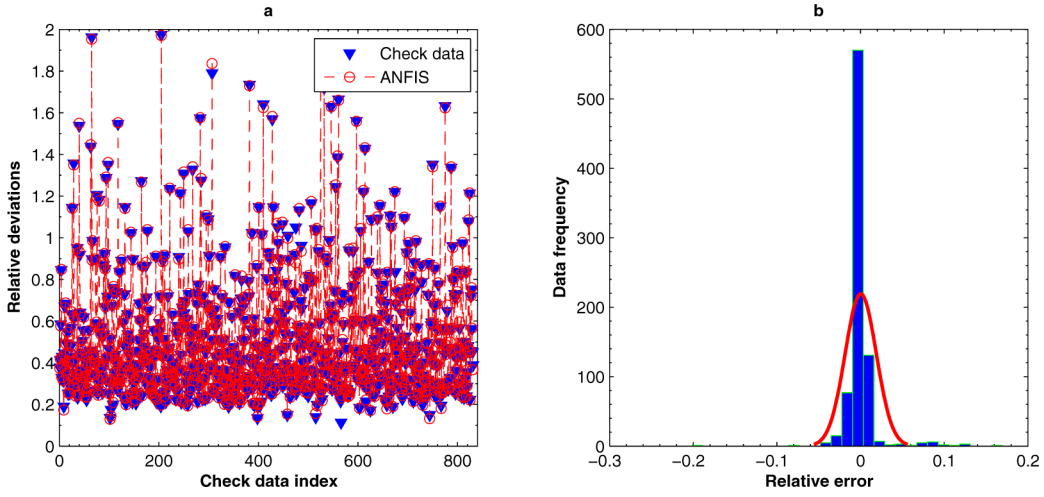

Figure 9. Deviations of ANFIS predictions from experimental data for the check set: (a) relative deviations, (b) error distributions histogram.

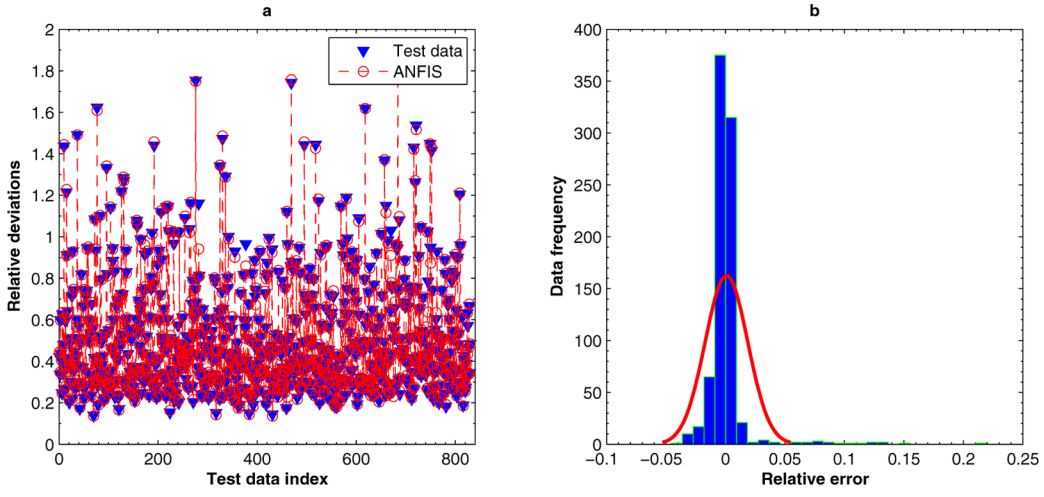

Figure 10. Deviations of ANFIS predictions from experimental data for the test set: (a) relative deviations, (b) error distributions histogram.

any offspring.[29] Individuals improved by the knowledge sharing property of PSO tend to produce better offspring than the original ones. Furthermore, computations of PSO are easy and add a slight computational burden when coupled with the GA, which in turn might also obviate the premature convergence of the individual PSO algorithm by mutating the stagnant particles.[29]

Taking into account the previous discussion on the merits and demerits of both algorithms, the hybrid of the GA and PSO appears to introduce a maturing property into the population from the GA perspective and increase diversity among the individuals from the PSO perspective so that the evolution of individuals is no longer restricted to be in the same generation.

dx.doi.org/10.1021/ie501702z | Ind. Eng. Chem. Res. XXXX, XXX, XXX−XXX

Table 3. Statistical Parameters of the Proposed ANFIS Model

statistical parameters	
Train Set	
R^{2a}	0.9989
average absolute error[b]	1.51
standard deviation error[c]	0.01424
root mean squared error[d]	0.0002026
N	3876
Check Set	
R^2	0.9981
average absolute error	1.93
standard deviation error	0.01866
root mean squared error	0.000348
N	831
Test Set	
R^2	0.9980
average absolute error	1.62
standard deviation error	0.01795
root mean squared error	0.0003225
N	830
Total	
R^2	0.9986
average absolute error	1.59
standard deviation error	0.01557
root mean squared error	0.0002424
N	5537

[a] $R^2 = 1 - ((\sum_i^N(\text{pred}(i) - \exp(i))^2)/(\sum_i^N(\text{pred} - \text{average}(\exp(i)))^2)$. [b] AAE, % = $((100)/(N))\sum_i^N((|\text{pred}(i) - \exp(i)|)/(\exp(i)))$. [c] SDE = $\sum_i^N(((\text{error}(i) - \text{average}(\text{error}(i)))^2)/(N))^{1/2}$. [d] RMSE = $((\sum_i^N(\text{pred}(i) - \exp(i))^2)/(N)^{1/2})$.

Figure 2 shows a schematic flowchart of the HGAPSO algorithm employed in this study for tuning the clustering radius.[38,39] More information on the hybrid smart techniques can be found in ref 38 and ref 39.

In the HGAPSO optimization algorithm, the position and velocity vectors hold a list of decision variables that must be optimized, which in this case is the effective clustering radius. In this work, optimization proceeds by minimizing the following cost function defined between the experimental data and the ANFIS predictions of the dynamic viscosity:

$$\text{cost} = \sqrt{\frac{1}{N}\sum_N (\mu_{\text{exp}} - \mu_{\text{pre}})^2} \quad (27)$$

where N defines the total number of data points, and the subscripts pre and exp denote the predicted and experimental dynamic viscosities, respectively.

At each iteration, a candidate radius is selected that has the best score among other candidates and is passed to the ANFIS. A hybrid learning algorithm is then used for improving the rate of convergence and optimizing the first order TSK and Gaussian MF parameters mentioned earlier. The ANFIS combines the least-squares and gradient descent methods, and the training process proceeds according to the algorithm designed in Figure 3.

4. RESULTS AND DISCUSSION

A top-down design algorithm represented in Figure 3 was devised to simulate viscosity values by the ANFIS model using the gathered experimental data. Since we were not aware of the optimum number of MFs, the SC method was initially used to select the optimum number of fuzzy sets for each input data. An HGAPSO algorithm was used to find the optimum clustering radius. This effective radius was obtained as 0.5064 after the termination of the optimization process. The determination of this optimum clustering radius led to the generation of 21 clusters for all input parameters according to the SC algorithm. The types of MFs were chosen to be Gaussian because of their smooth behavior and wide applicability.[22,24]

After the optimum clustering radius was found, the final ANFIS structure was then trained using the train data set and was validated by the check data set. Figure 4 indicates the final ANFIS structure together with its layers and a number of generated rules. The distribution of MFs generated for some input parameters including NaCl concentration, KCl concentration, temperature, and pressure are also shown in Figure 5. According to the nature of the SC algorithm, Gaussian MFs were distributed and concentrated around intervals with more recorded data and thus more diversity in the data set. The model was found to converge in less than 500 epochs using the optimum radius as indicated in Figure 6. Training and checking errors shown in this figure indicate no overfitting

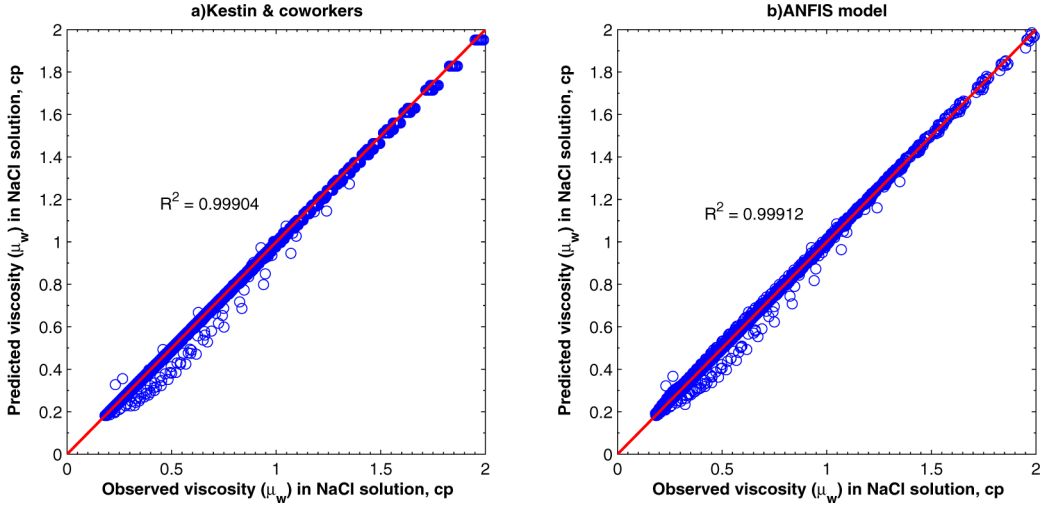

Figure 11. Predicted viscosity values in NaCl+H_2O solution versus experimental data for (a) Kestin and co-workers and (b) ANFIS model.

dx.doi.org/10.1021/ie501702z | Ind. Eng. Chem. Res. XXXX, XXX, XXX−XXX

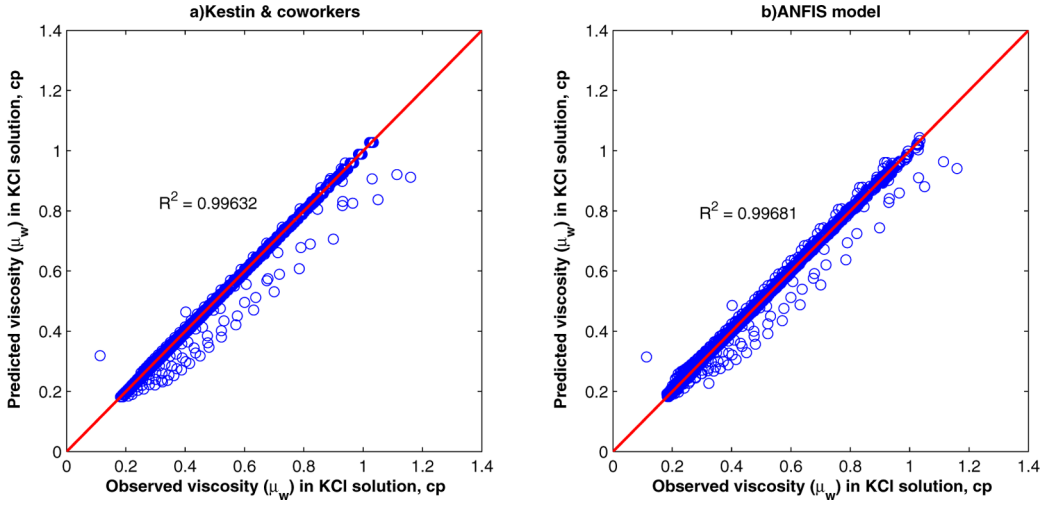

Figure 12. Predicted viscosity values in KCl+H_2O solution versus experimental data for (a) Kestin and co-workers and (b) ANFIS model.

during the training process as both follow approximately the same trends.

The constructed model for viscosity prediction was also compared to the experimental values for the train, check, and test sets shown in Figure 7. The concentration of points along the 45° line shows an excellent accordance between the model predictions and the observed experimental values. Figures 8−10 indicate the relative deviations and error distributions of the train, check, and test sets, respectively. Predicted viscosity values almost overlap with the experimentally recorded data, revealing a satisfactory agreement. Error distribution histograms also corroborate this accordance by showing a Gaussian normal distribution around zero. Statistical parameters showing model accuracy and robustness were also calculated. These parameters, which are the squared correlation coefficient (R^2), average absolute error (AAE), root mean squared error (RMSE), and standard deviation error (SDE) are summarized in Table 3. An overall correlation coefficient of 0.9986 and an average absolute error of 1.59% indicate excellent accordance between viscosity values predicted by the ANFIS and their respective experimental values. The overall RMSE value of 0.0002424 and SDE value of 0.01557 also support this acceptable match.

The dynamic viscosity values predicted by the ANFIS model were also compared with the empirical correlations previously mentioned in section 1.1 in their specified applicability ranges. Figures 11 and 12 represent the regression plots of the dynamic viscosity in NaCl and KCl binary solutions computed using the correlation presented by Kestin and co-workers[12,13] and then compared to the values predicted by the ANFIS model. These figures indicate that both the ANFIS model and this empirical correlation perform well but the ANFIS is slightly better.

These figures could be quite misleading and the ANFIS model appears to produce much better results when employing the same data interval. Statistical parameters calculated and summarized in Tables 4 and 5 for NaCl and KCl solutions, respectively, could elucidate and corroborate this fact even further. RMSE values calculated for the empirical correlations of Kestin and co-workers[12,13] are considerably large compared to those of the ANFIS model.

The proposed ANFIS model was also compared to the empirical correlation developed by Ershaghi, Abdassah, Bonakdar, and Ahmad[4] for NaCl salt-containing solutions in its specified thermodynamic range. Owing to the fact that this model does not account for the effect of pressure, only the portion of data at lower atmospheric pressures were singled out from among the large database gathered in this study. Regression plots are demonstrated in Figure 13 and pertinent statistical parameters are listed in Table 6. It is evident both numerically and graphically that the ANFIS model is superior over the empirical correlation of Ershaghi, Abdassah, Bonakdar, and Ahmad[4] when used for viscosity prediction over the same thermodynamic range.

According to the comparisons and testing results, the ANFIS proved to be more precise and reliable in contrast to the empirical equations available in the literature. The results obtained in this study justify the validity and reliability of this model while introducing it as an invaluable tool in research areas and simulations where knowledge of water viscosity of electrolyte solutions is of paramount importance. The observed deviations in the results of the empirical correlations could be attributed to the introduction of new experimental points and thus model parameters not being adjusted with respect to these new data points. Nevertheless, the main drawback to these empirical correlations is that they are only applicable to a certain salt and over a certain thermodynamic range.

Table 4. Statistical Parameters To Assess the Performance of ANFIS Model and Kestin and Co-workers Correlation in Predicting Viscosity of NaCl+H_2O Solution

statistical parameter	ANFIS model	Kestin and co-workers
R^2	0.99912	0.99904
average absolute error	1.4176	1.6964
standard deviation error	0.01416	14.8337
root mean squared error	0.0002024	16.9724
N	3125	3125

Table 5. Statistical Parameters To Assess the Performance of ANFIS Model and Kestin and Co-workers Correlation in Predicting Viscosity of KCl+H_2O Solution

statistical parameter	ANFIS model	Kestin and co-workers
R^2	0.99681	0.99632
average absolute error	1.5519	1.4922
standard deviation error	0.01617	17.3670
root mean squared error	0.0002614	17.8795
N	2603	2603

dx.doi.org/10.1021/ie501702z | Ind. Eng. Chem. Res. XXXX, XXX, XXX−XXX

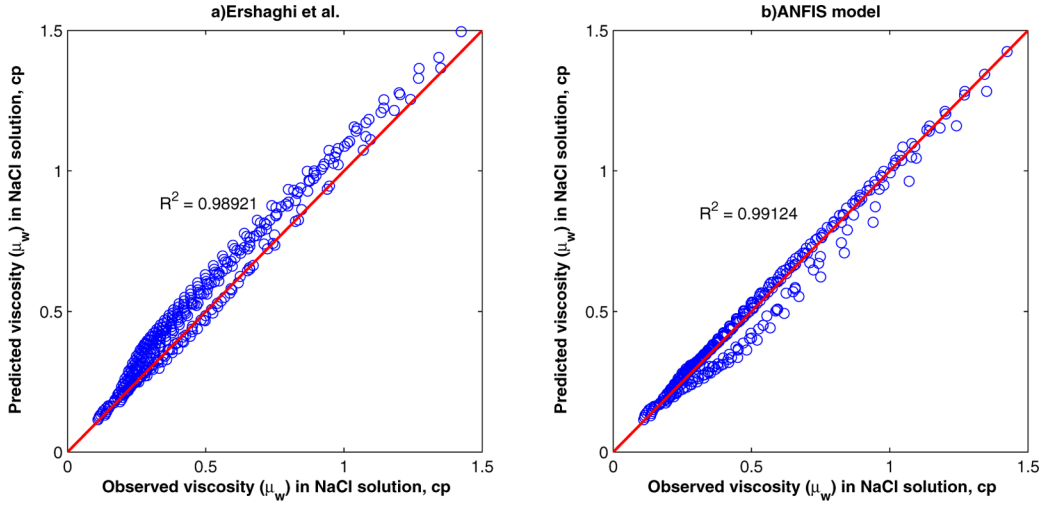

Figure 13. Predicted viscosity values in NaCl+H_2O solution versus experimental data for (a) Ershaghi et al. and (b) ANFIS model.

Table 6. Statistical Parameters To Assess the Performance of ANFIS Model and Ershaghi et al.'s Correlation in Predicting Viscosity of NaCl+H_2O Solution

statistical parameter	ANFIS model	Kestin and co-workers
R^2	0.991 24	0.98921
average absolute error	6.1747	13.6074
standard deviation error	0.0360	0.0446
root mean squared error	0.000 13	0.06929
N	399	399

On the other hand, the developed ANFIS model was observed to be capable of determining accurate dynamic viscosity values in multicomponent systems of NaCl, KCl, and $CaCl_2$ aqueous solutions. Although this model exhibited greater predictive performance compared to the previous multiple regression equations, it is important to design an appropriate ANFIS structure through a systematic way. In fact, heedless design of the ANFIS structure might lead to an increased number of tuning parameters and unnecessary system complexity and thus may result in overfitting.

5. CONCLUSIONS

Nowadays, multidisciplinary data integration techniques and soft computing approaches are successfully applied in solving a variety of complex engineering and science problems. In this work, the viscosities of aqueous chloride solutions were estimated using a hybrid of artificial neural networks and fuzzy logic termed as adaptive network-based fuzzy inference system (ANFIS). To provide a comprehensive database, an aggregate of 5537 experimental data was gathered from the open literature representing viscosity values over wide ranges of temperature, pressure, and salt compositions. The ANFIS structure was designed using the SC algorithm with an effective clustering radius optimized by the HGAPSO technique.

The optimization process resulted in an optimum number of 21 different clusters, which led to 21 distinct fuzzy if−then rules. After the ANFIS structure was successfully generated and tested, a comparison was drawn between the model predictions and real experimental data and a satisfactory agreement was observed giving a total R^2 value of 0.9986 and an AAE of 1.59%. The proposed model was also found to outperform multiple regression models presented by and Ershaghi, Abdassah, Bonakdar, and Ahmad[4] for a binary NaCl+H_2O system, and Kestin and co-workers[12,13] for binary NaCl+H_2O and KCl+H_2O solutions in their specified applicability ranges.

The constructed viscosity prediction model could successfully be applied in dynamic viscosity prediction of multicomponent (Na, K, or Ca)Cl−H_2O solutions over temperature ranges of 293.15−533.15 K and pressure ranges of 0.1−35 MPa. The developed model can also be integrated with commercial engineering software packages including CMG and ECLIPSE to increase their precision and reliability in accurately simulating the water flooding operations.

APPENDIX A: INSTRUCTION FOR USING THE DEVELOPED MODEL

To implement the developed ANFIS model, these instructions should be followed:

1) Assemble your own viscosity data set considering the input arrangements mentioned in eq 23.

```
load FIS;

Outputs=evalfis(Inputs,fis);
```

2) Export your data file into MATLAB workspace and load the FIS structure.
3) Type the following MATLAB code into debugger:

Example: Calculation of the water viscosity with the following sample data in Table AI.

Table AI. Sample Set for Calculation of Water Density

parameters	value
C_{NaCl}, m	3
C_{KCl}, m	0
C_{CaCl_2}, m	0
temperature, K	313.15
pressure, MPa	15

The output result of the program (based on the developed ANFIS model) will be 0.9008 cp while the corresponding experimental value is 0.9 cp.

Nomenclature

A, B = typical fuzzy sets
AAE = average absolute error, %

dx.doi.org/10.1021/ie501702z | Ind. Eng. Chem. Res. XXXX, XXX, XXX−XXX

ANFIS = adaptive network-based fuzzy inference system
ANN = artificial neural network
C = concentration, m
FCM = fuzzy c-means
FIS = fuzzy inference system
FL = fuzzy logic
Gb_i^j = global best of particle i at iteration j
MF = membership function
P = pressure, MPa
Pb_i^j = personal best of particle i at iteration j
R^2 = squared correlation coefficient
RMSE = root mean squared error
SC = subtractive clustering
SDE = standard deviation error
T = temperature, K
v = velocity vector
W = weight associated with each rule
w = inertia weight
X = input patterns
x = position vector
Y = output patterns
Z = Gaussian centers

Greek Symbols

β = membership degrees
μ = dynamic viscosity, cp
σ = standard deviation in Gaussian functions

AUTHOR INFORMATION

Corresponding Authors

*E-mail: safari.hossein68@gmail.com.
*E-mail: alireza.bahadori@scu.edu.au.

Notes

The authors declare no competing financial interest.

REFERENCES

(1) Francke, H.; Thorade, M. Density and Viscosity of Brine: An Overview from a Process Engineers Perspective. *Chem. Erde* **2010**, *70* (Suppl. 3, (0)), 23−32.
(2) Königsberger, E.; Königsberger, L. C.; May, P.; Harris, B. Properties of Electrolyte Solutions Relevant to High Concentration Chloride Leaching. II. Density, Viscosity, and Heat Capacity of Mixed Aqueous Solutions of Magnesium Chloride and Nickel Chloride Measured to 90 °C. *Hydrometallurgy* **2008**, *90* (2−4), 168−176.
(3) Abdulagatov, I. M.; Zeinalova, A.; Azizov, N. D. Viscosity of Aqueous Na_2SO_4 Solutions at Temperatures from 298 to 573 K and at Pressures up to 40 MPa. *Fluid Phase Equilib.* **2005**, *227* (1), 57−70.
(4) Ershaghi, I.; Abdassah, D.; Bonakdar, M.; Ahmad, S. Estimation of Geothermal Brine Viscosity. *J. Pet. Technol.* **1983**, *35*, 621−628.
(5) Ophori, D. U. Flow of Groundwater with Variable Density and Viscosity, Atikokan Research Area, Canada. *Hydrogeol. J.* **1998**, *6* (2), 193−203.
(6) Kestin, J.; Wang, H. Corrections for the Oscillating Disk Viscometer. *J. Appl. Mech.* **1957**, *79*, 197−206.
(7) Magri, F.; Bayer, U.; Clausnitzer, V.; Jahnke, C.; Diersch, H. J.; Fuhrmann, J.; Möller, P.; Pekdeger, A.; Tesmer, M.; Voigt, H. Deep Reaching Fluid Flow Close to Convective Instability in the NE German Basin—Results from Water Chemistry and Numerical Modelling. *Tectonophysics* **2005**, *397* (1−2), 5−20.
(8) Yidana, M. S. Groundwater Flow Modeling and Particle Tracking for Chemical Transport in the Southern Voltaian Aquifers. *Environ. Earth Sci.* **2011**, *63* (4), 709−721.
(9) Yidana, M. S.; Ophori, D.; Alo, C. A. Hydrogeological Characterization of a Tropical Crystalline Aquifer System. *J. Appl. Water Eng. Res.* **2014**, 1−12.
(10) Jamialahmadi, M.; Muller-Steinhagen, H. Mechanisms of Scale Deposition and Scale Removal in Porous Media. *Int. J. Oil, Gas Coal Technol.* **2008**, *1*, 81−108.
(11) Safari, H.; Jamialahmadi, M. Thermodynamics, Kinetics, and Hydrodynamics of Mixed Salt Precipitation in Porous Media: Model Development and Parameter Estimation. *Transp. Porous Media* **2014**, *101* (3), 477−505.
(12) Kestin, J.; Khalifa, H. E.; Correia, R. J. Tables of Dynamic and Kinematic Viscosity of Aqueous NaCl Solutions in the Temperature Range 20−150 °C and the Pressure Range 0.1−35 MPa. *Phys. Chem.* **1981**, *10* (1), 71−87.
(13) Kestin, J.; Khalifa, H. E.; Correia, R. J. Tables of Dynamic and Kinematic Viscosity of Aqueous KCl Solutions in the Temperature Range 25−150 °C and the Pressure Range 0.1−35 MPa. *Phys. Chem.* **1981**, *10* (1), 57−70.
(14) Numbere, D.; Bringham, W. E.; Standing, M. B. *Correlations for the Physical Properties of Petroleum Reservoir Brines*; Stanford University: Stanford, CA, 1977.
(15) Kestin, J.; Sokolov, M.; Wakeham, W. A. Viscosity of Liquid Water in the Range −8 to 150 °C. *J. Phys. Chem. Ref. Data* **1978**, *7*, 941.
(16) Swindells, J. F.; Coe, J. R.; Godfrey, T. B. Absolute Viscosity of Water at 20 °C. *J. Res. Natl. Bur. Stand.* **1952**, *48* (1), 1−31.
(17) Korosi, A.; Fabuss, B. M. Viscosities of Binary Aqueous Solutions of Sodium Chloride, Potassium Chloride, Sodium Sulfate, and Magnesium Sulfate at Concentrations and Temperatures of Interest in Desalination Processes. *J. Chem. Eng. Data* **1968**, *13* (4), 548−552.
(18) Bedrikovetsky, P.; Siqueira, F.; Furtado, C.; Souza, A. Modified Particle Detachment Model for Colloidal Transport in Porous Media. *Transp. Porous Media* **2011**, *86* (2), 353−383.
(19) Safari, H.; Gharagheizi, F.; Lemraski, A.; Jamialahmadi, M.; Mohammadi, A.; Ebrahimi, M. Rigorous Modeling of Gypsum Solubility in Na-Ca-Mg-Fe-Al-H-Cl-H2O System at Elevated Temperatures. *Neural Comput. Appl.* **2014**, 1−11.
(20) Eslamimanesh, A.; Gharagheizi, F.; Mohammadi, A. H.; Richon, D. Assessment Test of Sulfur Content of Gases. *Fuel Process. Technol.* **2013**, *110* (0), 133−140.
(21) Nikravesh, M.; Aminzadeh, F.; Zadeh, L. A. *Soft Computing and Intelligent Data Analysis in Oil Exploration*; Elsevier: Amsterdam, The Netherlands, 2003; Vol. *51*, pp 3−724, http://www.sciencedirect.com/science/book/9780444506856.
(22) Jang, J. S. R.; Sun, C. T.; Mizutani, E. *Neuro-Fuzzy and Soft Computing: A Computational Approach to Learning and Machine Intelligence*; Prentice Hall: Upper Saddle River, New Jersey, 1997.
(23) Lee, K. H. *First Course on Fuzzy Theory and Applications*; Springer: New York, 2005.
(24) Dursun, O. F.; Kaya, N.; Firat, M. Estimating Discharge Coefficient of Semi-elliptical Side Weir Using ANFIS. *J. Hydrol.* **2012**, *426−427* (0), 55−62.
(25) Tahseen, T. A.; Ishak, M.; Rahman, M. M. Performance Predictions of Laminar Heat Transfer and Pressure Drop in an In-Line Flat Tube Bundle Using an Adaptive Neuro-Fuzzy Inference System (ANFIS) Model. *Int. Commun. Heat Mass Transfer* **2014**, *50* (0), 85−97.
(26) Zadeh, L. A. Fuzzy Sets. *Inf. Control* **1965**, *8* (3), 338−353.
(27) Chiu, S. Fuzzy Model Identification Based on Cluster Estimation. *J. Intell. Fuzzy Syst.* **1994**, *2*, 267−278.
(28) Haupt, R. L.; Haupt, S. E. *Practical Genetic Algorithms*; Wiley: New York, 2004.
(29) Juang, C.-F. A Hybrid of Genetic Algorithm and Particle Swarm Optimization for Recurrent Network Design. *Trans. Syst. Man Cybern., Part B* **2004**, *34* (2), 997−1006.
(30) Wright, A. H. Genetic Algorithms for Real Parameter Optimization. *Found. Genet. Algorithms* **1991**, *1*, 205−218.
(31) Safari, H.; Jamialahmadi, M. Estimating the Kinetic Parameters Regarding Barium Sulfate Deposition in Porous Media: A Genetic Algorithm Approach. *Asia-Pac. J. Chem. Eng.* **2014**, *9* (2), 256−264.

(32) Eberhart, R.; Kennedy, J. In *A New Optimizer Using Particle Swarm Theory*, Proceedings of the Sixth International Symposium on Micro Machine and Human Science, 1995, MHS '95, 4−6 Oct 1995; IEEE: New York, 1995; pp 39−43.
(33) Poli, R.; Kennedy, J.; Blackwell, T. Particle Swarm Optimization. *Swarm Intell.* **2007**, *1* (1), 33−57.
(34) Shi, Y.; Eberhart, R. In *A Modified Particle Swarm Optimizer*, Evolutionary Computation Proceedings, 1998. IEEE World Congress on Computational Intelligence, The 1998 IEEE International Conference, 4−9 May 1998; IEEE: New York, 1998; pp 69−73.
(35) Shi, W.; Kan, A. T.; Fan, C.; Tomson, M. B. Solubility of Barite up to 250 °C and 1500 bar in up to 6 M NaCl Solution. *Ind. Eng. Chem. Res.* **2012**, *51* (7), 3119−3128.
(36) Van den Bergh, F.; Engelbrecht, A. P. A Cooperative Approach to Particle Swarm Optimization. *IEEE Trans. Evol. Comput.* **2004**, *8* (3), 225−239.
(37) Korosi, A.; Fabuss, B. M. Viscosity of Liquid Water from 25 to 150 Degree Measurements in Pressurized Glass Capillary Viscometer. *Anal. Chem.* **1968**, *40* (1), 157−162.
(38) Ahmadi, M. A.; Zendehboudi, S.; Lohi, A.; Elkamel, A.; Chatzis, I. Reservoir Permeability Prediction by Neural Networks combined with Hybrid Genetic Algorithm and Particle Swarm Optimization. *Geophys. Prospect.* **2013**, *61* (3), 582−598.
(39) Zendehboudi, S.; Ahmadi, M. A.; Mohammadzadeh, O.; Bahadori, A.; Chatzis, I. Thermodynamic Investigation of Asphaltene Precipitation During Primary Oil Production: Laboratory and Smart Technique. *Ind. Eng. Chem. Res.* **2013**, *52* (17), 6009−6031.